Electron probe micro analyser chemical zircon ages of the Khetri granitoids, Rajasthan, India: Records of widespread late Palaeoproterozoic extension-related magmatism

Parampreet Kaur[1], Naveen Chaudhri[1,*], S. Biju-Sekhar[2] and K. Yokoyama[3]

[1]Centre of Advanced Study in Geology, Panjab University, Chandigarh 160 014, India
[2]Institute of Geoscience, University of Tsukuba, Ibaraki 305-8571, Japan
[3]Department of Geology, National Science Museum, Hyakunin-cho, Shinjuku-ku, Tokyo 169 0073, Japan

A number of granitoid plutons were emplaced in the northernmost entity of the Aravalli craton, the Khetri Copper Belt (KCB). We report here Th–U–Pb electron probe micro analyser chemical ages for zircon and monazite from two granitoid plutons of the north KCB, the Biharipur and Dabla. Zircons occurring in the granitoids depict well-developed magmatic zoning and are chronologically unzoned. Both the plutons and their diverse granitoid facies are coeval and provide ages around 1765–1710 Ma. Geochemical attributes of the studied plutons are typical of A-type within-plate granites and consistent with an extensional tectonic environment. Our new age data are comparable to the petrologically similar A-type granitoids of the Alwar region, which have provided zircon chemical ages around 1780–1710 Ma. These analogous ages imply a widespread late palaeoproterozoic extension-related plutonism in the northern part of the Aravalli craton. The monazites, which were recovered only from the mafic magmatic rocks of the Biharipur pluton, yielded an isochron age of 910 ± 10 Ma, signifying an overprint of a younger Neoproterozoic thermal event in the region.

Keywords: Chemical ages, granitoid plutons, monazites, zircons.

THE most prominent physiographic feature of the Rajasthan craton is the NNE-SSW trending, ca. 800 km long Aravalli mountain range in the northwest peninsular India that preserves signatures of diverse geological and tectonic events from early Archaean to Recent. The basement Banded Gneissic Complex (circa 3.5 Ga) overlain by the cover sequences of Proterozoic linear supracrustal belts of Aravalli and Delhi fold belts, forms the basic geological framework for the Precambrian terrane of Rajasthan[1–3]. The Delhi Fold Belt is divided into two parts: an older segment to the north of Ajmer, the North Delhi Fold Belt (1800–1500 Ma)[4–6] and the relatively younger terrane to the south of Ajmer, the South Delhi Fold Belt (1000–850 Ma)[4,7]. From east to west, the North Delhi Fold Belt is splayed into three main sedimentary domains, the Bayana-Lalsot, the Alwar and the Khetri basins[8].

Till recently, most of the geochronological information in the North Delhi Fold Belt had been in the form of imprecise Rb–Sr whole-rock ages[4,9]. Crawford[9] was the first to provide the Rb–Sr data (model ages) of the two plutons from the Alwar basin, namely the Bairat granite (1660 Ma) and the Dadikar granite (2200 Ma), as well as one pluton from the Khetri Copper Belt (KCB), the Chapoli granite (1010 Ma). Subsequently, Gopalan *et al.*[10] reported a combined whole-rock Rb–Sr age of 1480 ± 40 Ma for two plutons (Saladipura and Udaipurwati) of the KCB. Choudhary *et al.*[4] dated the Harsora, Dadikar, Bairat and Ajitgarh granitoids of the Alwar basin, and the Sewli granitoids of the KCB. In the Rb–Sr isochron plot, the datapoints fall between two reference isochrons at 1500 and 1700 Ma. Deb *et al.*[5] suggested a Pb–Pb model age of ca. 1800 Ma for the Saladipura sulphide deposits of the KCB. An unpublished report of the BRGM[11] (vide Gupta *et al.*[12]) mentions single zircon ages of ca. 1700 Ma for the Gothara pluton, 1844 ± 7 Ma for the Jasrapura pluton and 1832 ± 3 Ma for the felsic volcanics of the Shyamgarh region. Sivaraman and Raval[13] provided 1680 ± 12 Ma U–Pb zircon concordia age for the Chapoli granite of the KCB. Recently, the Alwar granitoids have been chemically dated using an electron microprobe[6,14], and yielded ages around 1780–1710 Ma. These authors have also dated the Udaipurwati pluton of the KCB by the same method, at 1700–1680 Ma.

It should be noted that the major geochronological information obtained for the Khetri basin is from its southern segment. The existing age data for its northern segment are scarce, as no published radiometric ages are available except for those mentioned in the BRGM report[11]. The aim of this work is to present the EPMA chemical ages of zircons from the two granitoid plutons of the north KCB. In addition, we also report monazite ages from the mafic magmatic rocks. The results are further discussed and

*For correspondence. (e-mail: naveen.geol@gmail.com)

compared with those of the Alwar granitoids, to put constraints on the tectonic evolution of this terrane.

Geological setting

The KCB forms the northernmost entity of the Aravalli mountain range and extends for about 80 km from Singhana in the NE to Sangarva in the SW (Figure 1). The belt is further separated into the North KCB (NKCB) and the South KCB (SKCB) along the NW–SE striking transverse Kantli Fault[12]. The NKCB terrane is characterized by a multiphase structural history, magmatism, metamorphism and copper mineralization. Following Heron[15], Das Gupta[16] considered that the KCB is covered by rocks of the Delhi Supergroup, which is further divided into (1) an older psammitic dominated Alwar Group and (2) a younger pelitic dominated Ajabgarh Group (Figure 1). However, recent studies[17] assign a pre-Delhi status for the rocks of the KCB. Gupta *et al.*[12] have presented the stratigraphic and structural framework of the area in terms of Archaean (?) basement – Proterozoic cover sequences.

The metasedimentary rocks (feldspathic quartzite with magnetite, banded amphibole-quartzite, garnetiferous chlorite-schists, mica schists and quartzite) of the NKCB display a NNE–SSW to NE–SW trend and are folded into a number of regional anticlines and synclines, with culminations and depressions[16,18]. Metasediments of the KCB display two episodes (M_1 and M_2) of prograde regional metamorphism, the andalusite–sillimanite type of facies series in the north with a transition to kyanite–sillimanite type towards the south; there is an eastward increase in the grade of metamorphism[19,20].

The intrusive rocks in the KCB are largely represented by mafic and granitoid rocks. Ray[21] identified a 170 km long NNE–SSW trending lineament, the 'albitite line' in the region (Figure 1). Besides, minor amounts of felsic volcanics have also been reported[12,22]. The emplacement of most of the granitoid plutons was structurally controlled[12,16,23], and they occur in the cores of anticlines or parallel to foliation of the country rocks. These plutons have been interpreted as syn- to post-kinematic with respect to different episodes of the Delhi orogeny. Granitic activity in the KCB is considered to have taken place during the culmination of regional metamorphism[23]. The present work is concerned with the Biharipur and Dabla plutons of the NKCB, which are located about 15 km southeast of Khetri (Figure 1).

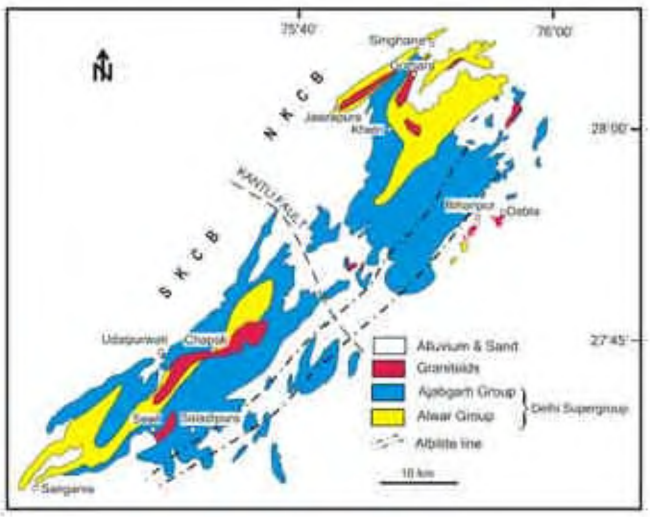

Figure 1. Geological map of the Khetri Copper Belt, showing location of Biharipur–Dabla and other granitoid plutons (compiled after Heron[15]; Ray[21]; Gupta *et al.*[12] and our own observations). SKCB, South Khetri Copper Belt; NKCB, North Khetri Copper Belt.

Field relationships, petrography and geochemistry

The Biharipur pluton occurs as a small-elongated body (ca. 2.0 km × 1.0 km) to the south of Biharipur village (Figure 1). The intrusive is essentially composed of two types of amphibole-bearing alkali–feldspar granites. The most dominant facies is the pink coloured, foliated microcline–albite granite (referred to as granite), which occupies the axial portion of the pluton and is in sharp contact with the albite granite. The albite granite, which is largely confined to the lower portions of the pluton, is white in colour, foliated and shows extensive commingling with the mafic magmatic rocks. Microgranite forms the subordinate facies, and occurs as pink-coloured dykes within granite and albite granite. Granite and albite granite are medium-grained, whereas microgranite is relatively fine-grained, and all the facies show hypidiomorphic granular texture. The granite and microgranite consist of quartz, microcline, albite, hastingsite amphibole and sometimes biotite. The albite granite is characterized by albite, quartz, actinolite amphibole, minor microcline and biotite. The accessory phases in the divergent granitoid facies include titanite, zircon, fluorite, apatite, magnetite, hematite, allanite, epidote and calcite.

The Dabla intrusive, which is an irregular-shaped granitoid body of ca. 1.8 km × 1.5 km, is exposed amidst the Quaternary sand and alluvium (Figure 1). Petrological details of the pluton are presented elsewhere[24]. Like Biharipur, it is also characterized by amphibole-bearing alkali–feldspar granites (microcline–albite granite, albite granite and microgranite) and displays similar field relations. However, unlike Biharipur, the granitoid facies of the Dabla do not exhibit foliation and mafic–albite granite commingled zones. Here, the plagioclase in the granite and albite granite is also virtually pure albite. The granite is characterized by hastingsite amphibole and locally contains hedenbergite and andradite, whereas actinolite (to ferro-actinolite) is present in albite granite. The microgranite facies is volumetrically less developed in Dabla compared to the Biharipur pluton.

Chemically, the albite granite and granite (including microgranite) of these plutons can be distinguished by

conspicuous disparity of alkali contents in the albite granite. The latter is characterized by remarkably low K_2O (< 1.0 wt%) and high Na_2O (~ 7.0 wt%) abundances compared to the granite at nearly constant SiO_2 levels. For other elements, there are no striking differences between albite granite and granite. Most of the granitoids have silica content > 70 wt%, suggesting highly evolved nature of these plutons. The studied granitoids are alkaline metaluminous to weakly peraluminous, ferroan and calc–alkalic in compositions. These geochemical attributes together with the Fe-rich nature of amphibole and biotite, high Ga/Al ratios, elevated concentrations of HFSE (Zr, Nb and Y) and REE, and lower abundances of CaO, MgO, Cr, Co, Ni, Sr and Eu serve to classify the rocks as typical A-type[25–28] within-plate[29] granites.

Analytical procedure

Application of Electron Probe Micro Analyser (EPMA) in the dating of zircon and monazite appears to be a promising technique and has been applied to igneous and metamorphic rocks[6,30–35]. This method has proved to be a valuable tool for geochronologists because of its low cost and high spatial resolution (≤ 5 μm), which is smaller than the smallest possible spot size of a sensitive high-resolution ion microprobe (SHRIMP) and considerably smaller than the samples that are analysed by the U–Th–Pb isotope dilution thermal ionization mass spectrometric method. The high spatial resolution of the method allows to carry out a large number of analyses in a single zircon crystal. Thus one can detect age and compositional inhomogeneity and zonation on a smaller scale[36]. The precision and sensitivity of the EPMA method is one order magnitude lower than other zircon dating techniques. This method cannot be applied to U-poor or younger zircons. Since the granitoids from northwest India are Proterozoic in age and contain UO_2-rich zircons, the uncertainties obtained[6,14] by linear regression lines were between ± 20 and ± 50 Ma.

The powdered samples (<60-mesh size) were cleaned using water to remove the dust particles. The fine-grained fraction obtained after cleaning was dried and magnetic minerals were removed using hand magnet. Heavy non-magnetic minerals in fraction were separated using heavy liquids and an isodynamic magnetic separator. The collected heavy fractions, including zircon and monazite, were mounted on a glass slide using epoxy resin and subjected to diamond-polishing. Zircon is common in the heavy fraction from granitoid samples, whereas monazite is only recovered from the Biharipur mafics which are commingled with the albite granites.

The theoretical concept of this study follows the chemical thorium–uranium–total Pb isochron method of Suzuki *et al.*[30], which is summarized below.

Initially, the apparent age (t) is calculated from each set of the UO_2, ThO_2 and PbO analyses (wt %) by solving the equation:

$$\frac{\mathrm{PbO}}{W_{\mathrm{Pb}}} = \frac{\mathrm{ThO_2}}{W_{\mathrm{Th}}}\{\exp(\lambda_{232}t)-1\} + \frac{\mathrm{UO_2}}{W_{\mathrm{U}}}\left[\frac{\exp(\lambda_{235}t)+138\exp(\lambda_{238}t)}{139}-1\right], \quad (1)$$

where W represents the gram-molecular weight of each oxide (W_{Pb} = 223.2, W_{Th} = 264.04 and W_U = 270.03) and λ indicates the decay constant of each isotope (λ_{232} = 4.9475×10^{-11}/yr, $\lambda_{235} = 9.8485 \times 10^{-10}$/yr and $\lambda_{238} = 1.5512 \times 10^{-10}$/yr)[37]. To eliminate the effect of variations in the Th/U ratio on total Pb produced over a given time span, the sum of ThO_2 and UO_2 is converted into ThO_2^* by:

$$\mathrm{ThO_2^*} = \mathrm{ThO_2} + \frac{\mathrm{UO_2}W_{\mathrm{Th}}}{W_{\mathrm{U}}\{\exp(\lambda_{232}t)-1\}}\left[\frac{\exp[\lambda_{235}t)+138\exp(\lambda_{238}t)}{139}-1\right]. \quad (2)$$

The best-fit regression line is determined by the procedure of York[38], taking into account the uncertainties in microprobe analysis, and calculating the first approximation of age (T) from the slope (m) of the following equation:

$$T = \frac{1}{\lambda_{232}}\ln\left[1+m\times\frac{W_{\mathrm{Th}}}{W_{\mathrm{Pb}}}\right], \quad (3)$$

and

$$m = \frac{\mathrm{PbO}}{\mathrm{ThO_2^*}}. \quad (4)$$

Following this, the second approximation is to replace the apparent ages (t) of eq. (2) with the first approximation (T) and calculate the ThO_2^{*2}, and get T_2 using eq. (3), with ThO_2^{*2} in place of ThO_2^*. The same procedure is repeated n times until the difference between T_n and T_{n-1} becomes negligible. Suzuki and Adachi[31] obtained both initial PbO content and age from the regression line on the PbO–ThO_2^* diagram, assuming that initial PbO is homogeneously present in the mineral. Recent studies have shown that the initial PbO is negligible in comparison with radiogenic Pb[33]. Hence in this study, the ages have been calculated assuming that initial Pb is zero.

Analyses of polished zircon and monazite fractions were made on a JEOL electron microprobe (JXA-8800) at the National Science Museum, Tokyo. The electron microprobe was equipped with four-wavelength dispersive-type spectrometers. The operating conditions were 15 kV accelerating voltage and 2 μm probe diameter. The probe current for zircon and monazite was 0.5 and 0.2 μA respectively. In this method, PRZ corrections (modified ZAF) were applied. Seven elements for zircon (Si, Zr, Y, Hf, U,

Table 1. Representative microprobe analyses (wt%) of zircons from various granite phases of the Biharipur pluton. Error (1σ) for each analysis is also shown

UO_2	ThO_2	PbO	Age (Ma)	Error age (Ma)	ThO_2^*	UO_2	ThO_2	PbO	Age (Ma)	Error age (Ma)	ThO_2^*
BH-24											
0.509	0.142	0.152	1721	27	2.022	0.182	0.112	0.058	1690	70	0.780
0.495	0.170	0.153	1748	28	2.005	0.166	0.162	0.060	1769	71	0.780
0.455	0.129	0.140	1767	31	1.819	0.166	0.129	0.060	1835	75	0.750
0.391	0.110	0.123	1802	36	1.566	0.146	0.015	0.043	1760	98	0.555
0.390	0.045	0.114	1748	37	1.490	0.144	0.108	0.048	1709	86	0.638
0.384	0.059	0.109	1698	37	1.473	0.143	0.023	0.043	1764	99	0.556
0.336	0.195	0.109	1737	39	1.437	0.127	0.124	0.050	1887	93	0.603
0.331	0.245	0.111	1736	38	1.468	0.109	0.065	0.037	1801	118	0.470
0.253	0.052	0.077	1780	56	0.992	0.095	0.098	0.036	1807	123	0.452
0.248	0.177	0.090	1861	51	1.108	BH-67					
0.241	0.200	0.086	1793	51	1.096	0.372	0.231	0.126	1785	35	1.614
0.218	0.062	0.068	1779	63	0.871	0.294	0.077	0.090	1762	47	1.169
0.213	0.171	0.073	1736	58	0.960	0.213	0.064	0.068	1815	65	0.857
0.195	0.164	0.071	1814	63	0.893	0.197	0.049	0.059	1732	71	0.777
0.182	0.032	0.051	1669	77	0.702	0.154	0.055	0.045	1675	88	0.620
0.175	0.057	0.058	1869	78	0.713	0.153	0.105	0.052	1762	82	0.671
0.174	0.115	0.054	1634	72	0.754	0.139	0.141	0.051	1773	84	0.657
0.156	0.060	0.052	1837	87	0.642	0.139	0.054	0.046	1839	97	0.573
BH-43						0.138	0.046	0.044	1787	99	0.559
0.343	0.118	0.109	1783	40	1.395	0.135	0.010	0.040	1794	107	0.512
0.296	0.206	0.100	1761	43	1.306	0.132	0.089	0.052	1989	97	0.592
0.322	0.068	0.087	1605	43	1.245	0.105	0.008	0.031	1803	137	0.399
0.283	0.082	0.085	1726	49	1.129	0.099	0.028	0.030	1750	138	0.396
0.245	0.172	0.081	1727	51	1.078	BH-52					
0.243	0.163	0.081	1739	52	1.064	0.602	0.435	0.201	1731	21	2.662
0.247	0.153	0.080	1722	52	1.064	0.575	0.441	0.198	1760	22	2.575
0.243	0.112	0.079	1773	55	1.013	0.552	0.347	0.188	1793	24	2.403
0.209	0.159	0.074	1806	60	0.940	0.532	0.379	0.178	1736	24	2.346
0.212	0.086	0.067	1755	63	0.872	0.514	0.326	0.169	1736	25	2.227
0.221	0.061	0.066	1718	63	0.876	0.513	0.365	0.172	1737	25	2.263
0.233	0.041	0.066	1677	61	0.898	0.471	0.248	0.152	1741	28	1.994
0.206	0.051	0.063	1758	68	0.815	0.449	0.197	0.142	1749	30	1.859
0.177	0.120	0.061	1798	71	0.781	0.446	0.289	0.146	1725	29	1.936
0.131	0.112	0.045	1734	93	0.595	0.432	0.246	0.140	1741	30	1.844
0.143	0.036	0.044	1760	97	0.567	0.414	0.212	0.133	1746	32	1.747
0.140	0.011	0.043	1835	103	0.534	0.400	0.231	0.130	1744	33	1.712
0.120	0.036	0.039	1816	114	0.485	0.381	0.215	0.124	1751	34	1.628
0.123	0.006	0.036	1797	118	0.464	0.379	0.209	0.121	1723	35	1.611
BH-8						0.378	0.187	0.122	1758	35	1.588
0.410	0.384	0.148	1777	30	1.910	0.358	0.189	0.116	1751	37	1.515
0.281	0.037	0.085	1801	51	1.085	0.349	0.151	0.119	1856	39	1.458
0.250	0.232	0.091	1788	48	1.162	0.349	0.202	0.113	1739	37	1.492
0.246	0.194	0.087	1786	51	1.108	0.347	0.220	0.112	1709	37	1.501
0.215	0.047	0.059	1619	65	0.833	0.342	0.210	0.114	1768	38	1.481
0.206	0.273	0.086	1876	54	1.047	0.299	0.127	0.096	1766	45	1.238

Th, Pb) and 14 elements for monazite (P, Si, La, Ce, Pr, Nd, Sm, Gd, Dy, Y, U, Th, Pb, Ca) were analysed to check their structural formulae and total concentration. The synthetic minerals γUO_3 and ThO_2, and natural $PbCrO_3$ were used as standards for measuring the weight percentage of U, Th and Pb respectively. Age calibrations were performed by comparing ages of zircons and monazites as obtained from EPMA and those generated by SHRIMP technique[6,35]. These were found to be well consistent. Least square fitting was applied to calculate the age for a linear regression line with an assumption that each dataset belongs to a single thermal event.

Errors and data presentation

Errors of UO_2, ThO_2 and PbO measurements are calculated using counting statistics in X-ray analyses. Although the age for each measurement is computed from the complex equations[31,33,39], error of the age is calculated by the following simplified equation originally developed by Holmes[40]:

$$\text{Age (Ma)} = a^*(\text{PbO})/\{(\text{UO}_2) + b^*(\text{ThO}_2)\}.$$

In this equation, each element is shown as an oxide wt%. The values of factors a and b vary from 3.3 and 23500 at

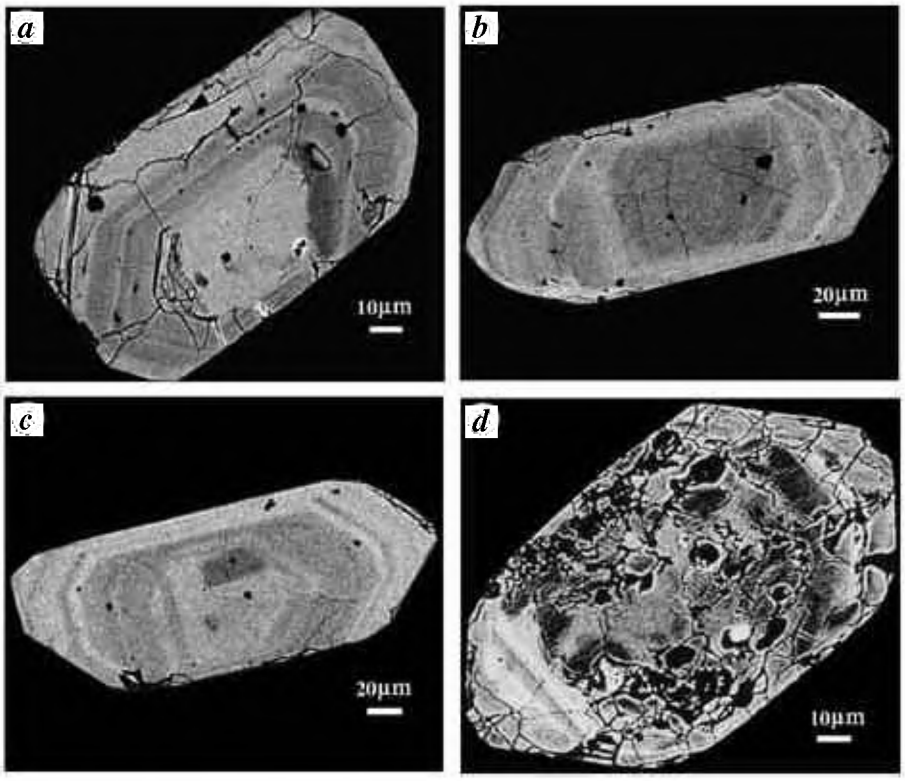

Figure 2. Back scattered electron images of zircons from Biharipur and Dabla plutons. ***a***, Zircon from Biharipur granite facies depicting magmatic zoning and development of cracks. ***b***, ***c***, Dabla granite zircons showing euhedral shape and well-developed magmatic zoning. ***d***, U-rich zircon of Biharipur granite facies showing metamictization.

500 Ma to 4.0 and 22000 at 2500 Ma respectively. The uncertainty on the age of each analytical point is calculated by propagating the uncertainties on UO_2, ThO_2 and PbO into the simplified equation above. Here, only error of age is given in the tables at the 1-sigma (1σ) confidence level. As peak and background ratios of trace elements are low, errors of UO_2, ThO_2 and PbO in zircon are roughly constant, around 0.0032, 0.0054 and 0.0021 wt% respectively. In monazite, errors of UO_2, ThO_2 and PbO are 0.088, 0.027, 0.039 wt%, respectively. Although error of ThO_2 changes with its amount, age error in monazite is almost totally controlled by the error of PbO content.

The zircon analyses were performed on 5 and 4 representative samples of granitoids from Biharipur and Dabla plutons respectively. These include two granite, two albite granite and one sample of microgranite from Biharipur, whereas three granites and one albite granite have been selected from the Dabla pluton. Representative UO_2, ThO_2 and PbO concentrations of zircons along with ThO_2^* and age data (in Ma) of the Biharipur and Dabla granitoids are listed in Tables 1 and 2 respectively.

Results and discussion

The back scattered electron (BSE) images were used for evaluating and understanding the internal structure of zircons. Representative BSE images of zircon from each pluton are shown in Figure 2. Zircons from both the plutons are mainly euhedral in shape and show compositional magmatic zoning (Figure 2 *a–c*). Some of the euhedral zircons in these plutons exhibit fractures and in some, the U-rich domains have undergone metamictization (Figure 2 *d*). Zircons with well-developed magmatic zoning were selected for age determination, and multiple zircon grains were analysed. The chemical compositions of zircon were mainly determined along their bright-coloured portions. The ages obtained from both rim and core portions were homogeneous. The Th–U–Pb system in zircon can be occasionally disrupted by partial Pb loss. However, a linear array on the PbO–ThO_2^* diagrams (Figures 3 and 4) precludes such a possibility in the present case and points to a closed system behaviour[41].

For the Biharipur pluton, all three granitoid facies were analysed. Two samples of the granite yield similar ages within the error; sample BH-43 provides an age of 1710 ± 40 Ma, and the obtained age for BH-24 is 1750 ± 20 Ma. Datapoints of analysed euhedral zircon grains of these samples are linearly arranged in the ThO_2^* versus PbO isochron plots (Figure 3). Zircons from two samples of the Biharipur albite granite have yielded nearly identical ages; sample BH-8 shows an age of 1760 ± 30 Ma, while BH-67 gives an age of 1765 ± 30 Ma. All datapoints display remarkable linear arrays in similar isochron plots

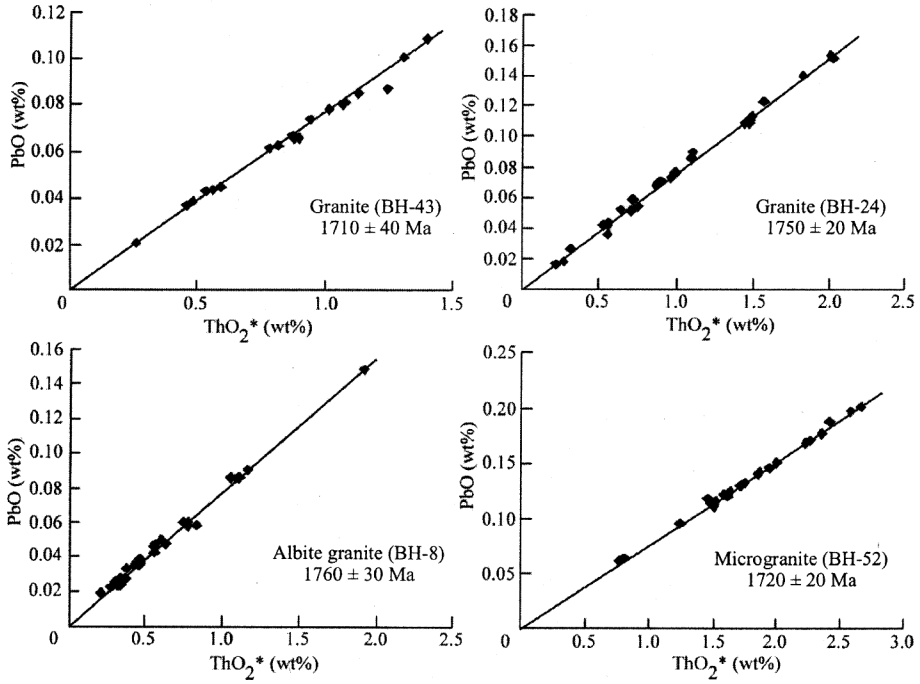

Figure 3. PbO versus ThO_2^* plots showing isochrons of zircon data of Biharipur pluton.

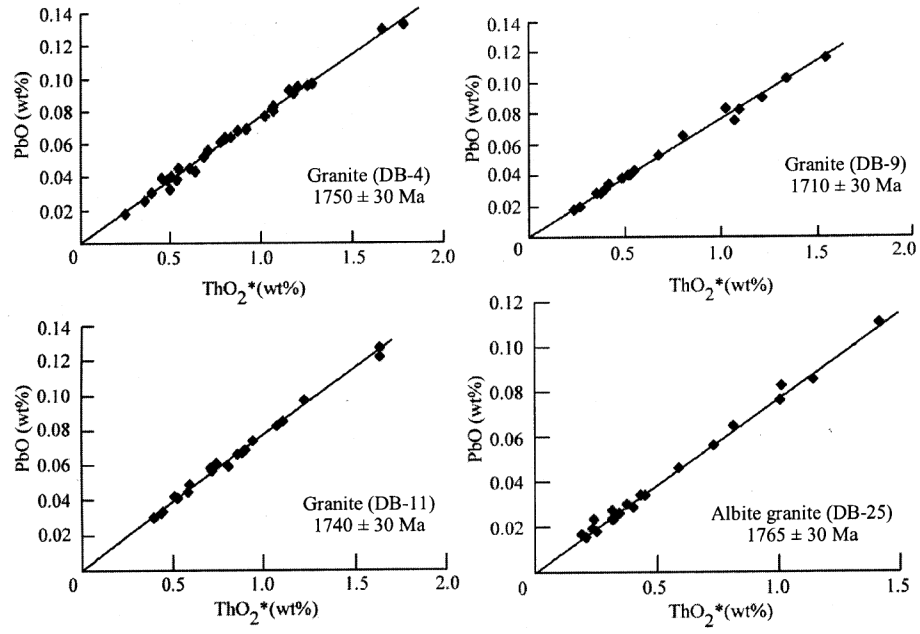

Figure 4. PbO versus ThO_2^* plots showing isochrons of zircon data of Dabla pluton.

(Figure 3). The Biharipur microgranite sample BH-52 is also characterized by a well-defined linear array (Figure 3) and records an age of 1720 ± 20 Ma.

Samples analysed from the Dabla pluton include those of granite and albite granite. Like Biharipur, zircons from four Dabla granite samples are also arrayed linearly on the ThO_2^* versus PbO plots (Figure 4). The age data computed from EPMA analyses for zircons of the aforementioned samples have yielded sharply defined isochrons at 1750 ± 30 Ma (DB-4), 1710 ± 30 Ma (DB-9) and 1740 ± 30 Ma (DB-11). Datapoints from the albite granite sample (DB-25) of the Dabla pluton also define a good linear isochron age of 1765 ± 30 Ma (Figure 4).

Apart from zircons in granitoids, monazites from the mafic magmatic rocks of the Biharipur pluton were also analysed. Thirty-four analyses were performed from several

Table 2. Representative microprobe analyses (wt%) of zircons from various granite phases of the Dabla pluton. Error (1σ) for each analysis is also shown

UO_2	ThO_2	PbO	Age (Ma)	Error age (Ma)	ThO_2^*	UO_2	ThO_2	PbO	Age (Ma)	Error age (Ma)	ThO_2^*
DB-4											
0.389	0.346	0.133	1708	31	1.782	0.077	0.093	0.029	1730	145	0.377
0.360	0.325	0.130	1786	34	1.664	0.096	0.000	0.028	1797	152	0.358
0.293	0.195	0.097	1739	44	1.278	DB-11					
0.282	0.134	0.090	1755	47	1.180	0.366	0.283	0.122	1716	34	1.633
0.281	0.213	0.095	1740	44	1.254	0.346	0.354	0.127	1770	35	1.640
0.280	0.028	0.083	1779	51	1.070	0.279	0.177	0.097	1825	46	1.220
0.272	0.195	0.094	1788	47	1.206	0.253	0.169	0.085	1754	50	1.108
0.254	0.210	0.092	1818	49	1.160	0.238	0.195	0.083	1755	52	1.076
0.248	0.147	0.080	1731	52	1.063	0.238	0.021	0.069	1752	61	0.901
0.233	0.207	0.079	1704	52	1.068	0.218	0.128	0.074	1796	59	0.941
0.216	0.223	0.077	1729	54	1.022	0.209	0.112	0.067	1740	62	0.884
0.211	0.020	0.063	1790	68	0.804	0.204	0.104	0.066	1759	64	0.860
0.209	0.151	0.069	1717	60	0.921	0.194	0.094	0.059	1678	68	0.807
0.197	0.102	0.065	1773	67	0.833	0.187	0.043	0.061	1863	75	0.745
0.193	0.158	0.068	1771	64	0.877	0.172	0.079	0.057	1796	77	0.721
0.186	0.090	0.062	1797	71	0.783	0.158	0.120	0.058	1862	79	0.714
0.172	0.165	0.064	1813	69	0.808	0.145	0.051	0.045	1737	93	0.587
0.158	0.116	0.056	1816	79	0.707	0.139	0.072	0.049	1870	94	0.595
0.148	0.137	0.052	1740	81	0.685	0.115	0.082	0.042	1867	109	0.514
0.130	0.132	0.045	1704	90	0.612	0.115	0.010	0.033	1721	125	0.434
0.123	0.026	0.038	1798	113	0.486	0.112	0.030	0.034	1724	123	0.445
0.119	0.104	0.038	1631	101	0.538	0.105	0.012	0.030	1707	136	0.398
0.114	0.084	0.040	1799	109	0.509	0.098	0.161	0.041	1779	105	0.527
DB-9						DB-25					
0.330	0.326	0.117	1730	36	1.545	0.341	0.149	0.110	1783	40	1.416
0.338	0.081	0.103	1757	41	1.335	0.252	0.212	0.085	1712	49	1.143
0.320	0.030	0.090	1710	45	1.212	0.232	0.149	0.076	1731	55	1.006
0.237	0.138	0.083	1853	55	1.026	0.225	0.163	0.083	1871	56	1.010
0.261	0.131	0.082	1714	50	1.095	0.190	0.107	0.064	1807	68	0.814
0.283	0.041	0.075	1603	50	1.074	0.167	0.112	0.056	1757	76	0.730
0.180	0.128	0.066	1864	70	0.804	0.134	0.093	0.046	1789	94	0.591
0.158	0.090	0.053	1787	82	0.678	0.101	0.061	0.034	1782	127	0.435
0.130	0.070	0.043	1777	99	0.555	0.095	0.102	0.034	1733	121	0.452
0.117	0.081	0.040	1790	107	0.517	0.086	0.089	0.029	1631	134	0.404
0.126	0.067	0.040	1718	103	0.531	0.084	0.062	0.030	1846	148	0.375
0.112	0.068	0.038	1792	114	0.487	0.080	0.024	0.023	1668	169	0.320
0.095	0.059	0.034	1879	135	0.415	0.077	0.064	0.026	1713	157	0.347
0.083	0.097	0.032	1790	136	0.405	0.066	0.070	0.024	1710	173	0.315

monazite grains and twelve analyses were carried out on a single grain in order to delineate the age difference between core and rim, if any. However, uniform ages were obtained from the rim and core portions of this monazite grain (Figure 5 *a*). The ThO_2 concentrations of the analysed monazite grains range from 9.40 to 24.3 wt%, while UO_2 concentrations vary from 0.16 to 0.50 wt%, and those of PbO lie between 0.39 and 1.01 wt% (Table 3). Despite these variations, individual as well as single grains (core to rim) record largely uniform PbO/ThO_2^* ratios, suggesting monazite formation in a single thermal event. All data points, linearly arranged in a PbO–ThO_2^* diagram yielded an age of 910 ± 10 Ma (Figure 5 *b*). This age is much younger than that obtained from the zircons of granitoids, and the studied zircons do not show any overprint of this younger event. This might be related to the difference in closure temperatures of both the minerals, which in turn also depends on the size of the minerals[42]. The closure temperature of zircon is around 1000°C, whereas the same in monazite is usually lower, around 650°C at a size of 100 μm and 800°C at 1000 μm[42]. Hence, the monazite will be strongly reset by the thermal event, whereas zircon will preserve the original chemical compositions.

The ages of ca. 1750–1710 Ma obtained for the granite facies of Dabla pluton are comparable to those of the Biharipur granite ages (1750–1710 Ma). The albite granites of both the plutons also provided consistent ages of 1765–1760 Ma. The ages yielded from all the different facies of the Biharipur–Dabla intrusives thus define a range of 1765–1710 Ma and imply coeval nature of these granitoid plutons.

The granitoid rocks of the Alwar basin, which lies further southeast of the Khetri basin, have also yielded[6] comparable zircon chemical ages of 1780–1710 Ma. Like Biharipur

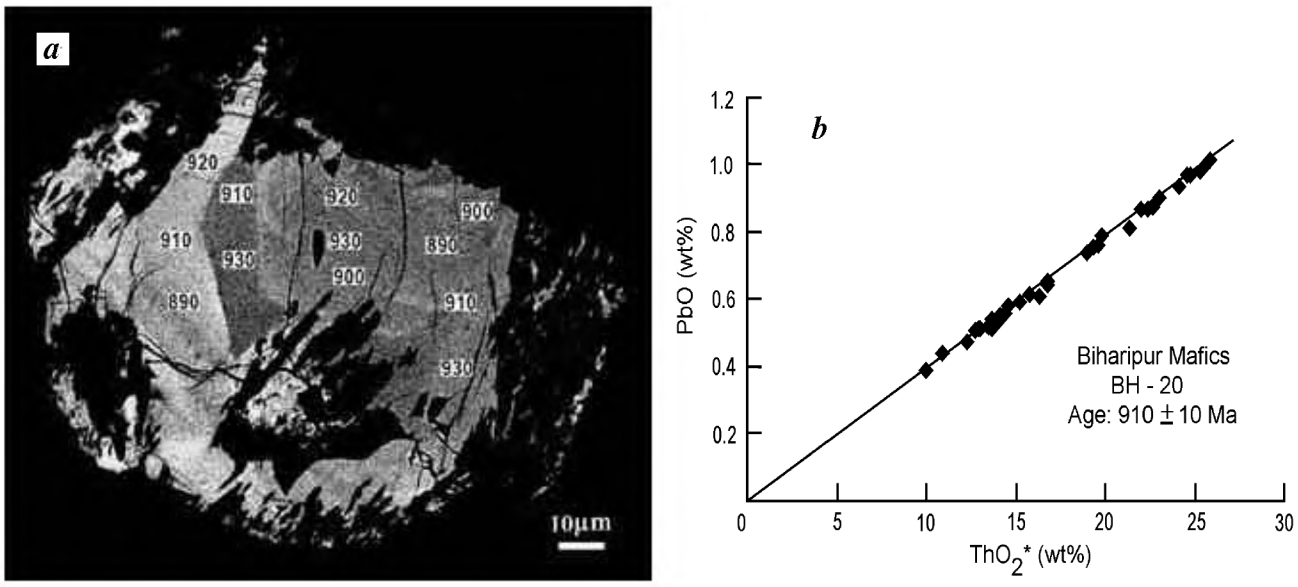

Figure 5. *a*, Back scattered electron image of a selected monazite grain from Biharipur mafic rocks. Numbers represent age values (in Ma) obtained in the various zones. *b*, PbO versus ThO_2^* plot for monazites showing isochron age.

Table 3. Electron microprobe analyses (wt%) of monazites from Biharipur mafics. Error (1σ) for each analysis is also shown

UO_2	ThO_2	PbO	Age (Ma)	Error age (Ma)	ThO_2^*
0.403	18.420	0.789	932	5	19.798
0.357	17.780	0.737	907	5	19.000
0.420	19.970	0.810	885	5	21.401
0.447	21.130	0.871	899	4	22.658
0.385	18.310	0.760	905	5	19.626
0.501	22.400	0.934	905	4	24.113
0.264	15.450	0.611	874	6	16.350
0.303	15.730	0.653	910	6	16.766
0.188	11.680	0.474	899	8	12.322
0.216	12.040	0.508	928	8	12.780
0.246	13.180	0.535	893	7	14.021
0.287	14.290	0.590	904	6	15.271
0.405	21.600	0.901	916	4	22.985
0.429	23.820	0.983	909	4	25.285
0.462	24.250	1.014	917	4	25.831
0.441	23.120	0.969	919	4	24.628
0.447	23.210	0.970	917	4	24.737
0.384	21.040	0.866	906	4	22.351
0.256	14.880	0.615	912	6	15.755
0.504	23.830	0.991	907	4	25.550
0.180	10.270	0.437	937	9	10.888
0.165	9.400	0.386	906	10	9.962
0.398	20.680	0.868	921	4	22.043
0.228	12.250	0.510	915	7	13.030
0.224	12.200	0.515	928	7	12.968
0.336	18.210	0.753	910	5	19.357
0.297	15.810	0.640	889	6	16.824
0.235	13.330	0.554	916	7	14.133
0.226	12.890	0.541	925	7	13.665
0.231	13.650	0.556	900	7	14.439
0.261	13.720	0.579	925	7	14.614
0.227	12.890	0.531	908	7	13.667
0.224	12.930	0.514	878	7	13.692
0.228	12.710	0.521	903	7	13.488

and Dabla, the Alwar granitoids also exhibit signatures of A-type within-plate granites[6,43] and are thus similar in many respects with those of the NKCB granitoids. These analogous geochemical and geochronological characteristics of the granitoids of the two regions suggest a prominent and widespread late Palaeoproterozoic thermal event in the north DFB, and the A-type nature of this magmatism further implies that these plutons were emplaced in a region undergoing crustal extension.

Younger Neoproterozoic ages in this terrane have been reported in the form of Rb–Sr mineral isochron age from SKCB granitoids (850–700 Ma)[9,10]. The younger ages obtained from the monazites (ca. 910 Ma) of mafic rocks could be attributed to a younger thermal event, which resulted in the formation of new monazites. This younger thermal event may be correlated to the extensive magmatism that occurred[7,44] in the South Delhi Fold Belt at around 1000 Ma.

1. Gupta, S. N., Arora, Y. K., Mathur, R. K., Iqbaluddin, Prasad, B., Sahai, T. N. and Sharma, S. B., The Precambrian geology of the Aravalli region, southern Rajasthan and northeastern Gujarat. *Geol. Surv. India Mem.*, 1997, 123, p. 262.
2. Sinha-Roy, S. Malhotra, G. and Mohanty, M., In *Geology of Rajasthan*, Geological Society of India, Bangalore, 1998, p. 278.
3. Roy, A. B. and Jakhar, S. R., In *Geology of Rajasthan (Northwest India) Precambrian to Recent*, Scientific Publishers (India), Jodhpur, 2002, p. 421.
4. Choudhary, A. K., Gopalan, K. and Anjaneya Sastry, C., Present status of geochronology of the Precambrian rocks of Rajasthan. *Tectonophysics*, 1984, **105**, 131–140.
5. Deb, M., Thorpe, R. I., Cumming, G. L. and Wagner, P. A., Age, source and stratigraphic implications of Pb isotope data for conformable, sediment-hosted, base metal deposits in the Proterozoic Aravalli–Delhi orogenic belt, northwestern India. *Precambrian Res.*, 1989, **43**, 1–22.

6. Biju-Sekhar, S., Yokoyama, K., Pandit, M. K., Okudaira, T., Yoshida, M. and Santosh, M., Late Paleoproterozoic magmatism in Delhi Fold Belt, NW India and its implication: evidence from EPMA chemical ages of zircons. *J. Asian Earth Sci.*, 2003, **22**, 189–207.
7. Deb, M., Thorpe, R. I., Krstic, D., Corfu, F. and Davis, D. W., Zircon U–Pb and galena Pb isotope evidence for an approximate 1.0 Ga terrane constituting the western margin of the Aravalli–Delhi orogenic belt, northwestern India. *Precambrian Res.*, 2001, **108**, 195–213.
8. Singh, S. P., Stratigraphy and sedimentation pattern in the Proterozoic Delhi Supergroup, northwestern India. In *Precambrian of the Aravalli Mountain, Rajasthan, India* (ed. Roy, A. B.), Geol. Soc. India Mem., 1988, vol. 7, pp. 193–206.
9. Crawford, A. R., The Precambrian geochronology of Rajasthan and Bundelkhand, northern India. *Can. J. Earth Sci.*, 1970, **7**, 91–110.
10. Gopalan, K., Trivedi, J. R., Balasubramanyam, M. N., Ray, S. K. and Anjaneya Sastry, C., Rb–Sr chronology of the Khetri Copper Belt, Rajasthan. *J. Geol. Soc. India*, 1979, **20**, 450–456.
11. BRGM, AAP2-BRGM Report, R36979 DEX, 1993, DMM-93.
12. Gupta, P., Guha, D. B. and Chattopadhyay, B., Basement-cover relationship in the Khetri Copper Belt and the emplacement mechanism of the granite massifs, Rajasthan. *J. Geol. Soc. India*, 1998, **52**, 417–432.
13. Sivaraman, T. V. and Raval, U., U–Pb isotopic study of zircons from a few granitoids of Delhi–Aravalli Belt. *J. Geol. Soc. India*, 1995, **46**, 461–475.
14. Biju-Sekhar, S., Pandit, M. K., Yokoyama, K. and Santosh, M., Electron microprobe dating of the Ajitgarh and Barodiya granitoids, NW India: implications on the evolution of Delhi Fold Belt. *J. Geosci. Osaka City Univ.*, 2002, **45**, 13–27.
15. Heron, A. M., Geology of western Jaipur. *Geol. Surv. India, Rec.*, 1923, **54**, 345–397.
16. Das Gupta, S. P., The structural history of the Khetri Copper Belt, Jhunjhunu and Sikar districts, Rajasthan. *Geol. Surv. India Mem.*, 1968, 98, p. 170.
17. Chakrabarti, B. and Gupta, G. P., Stratigraphy and structure of the North Delhi Basin. *Geol. Surv. India, Rec.*, 1992, **124**, 5–9.
18. Naha, K., Mukhopadhyay, D. K. and Mohanty, R., Structural evolution of the rocks of the Delhi Group around Khetri, northeastern Rajasthan. In *Precambrian of the Aravalli Mountain, Rajasthan, India* (ed. Roy, A. B.), Geol. Soc. India, Mem., 1988, vol. 7, pp. 207–245.
19. Lal, R. K. and Shukla, R. S., Low-pressure regional metamorphism in the northern portion of the Khetri Copper Belt, Rajasthan, India. *Neues Jahrb. Mineral., Abh.*, 1975, **124**, 294–325.
20. Lal, R. K. and Ackermand, D., Phase petrology and polyphase andalusite-sillimanite type regional metamorphism in pelitic schist of the area around Akwali, Khetri Copper Belt, Rajasthan, India. *Neues Jahrb. Mineral., Abh.*, 1981, **141**, 161–185.
21. Ray, S. K., The albitite line of northern Rajasthan – a fossil intracontinental rift zone. *J. Geol. Soc. India*, 1990, **36**, 413–423.
22. Golani, P. R., Gathania, R. C., Grover, A. K. and Bhattacharjee, J., Felsic volcanics in South Khetri Belt, Rajasthan and their metallogenic significance. *J. Geol. Soc. India*, 1992, **40**, 79–87.
23. Bhattacharya, P. K. and Das Gupta, S., Evolution of the massive granites in the Khetri Copper Belt, Rajasthan: implication in regional correlation. *Indian J. Earth Sci.*, 1981, **8**, 44–53.
24. Chaudhri, N., Kaur, P., Okrusch, M. and Schimrosczyk, A., Characterisation of the Dabla granitoids, North Khetri Copper Belt, Rajasthan, India: evidence of bimodal anorogenic felsic magmatism. *Gondwana Res.*, 2003, **6**, 879–895.
25. Collins, B. J., Beams, S. D., White, A. J. R. and Chappell, B. W., Nature and origin of A-type granites with particular reference to southeastern Australia. *Contrib. Mineral. Petrol.*, 1982, **80**, 189–200.
26. Whalen, J. B., Currie, K. L. and Chappell, B. W., A-type granites: geochemical characteristics, discrimination and petrogenesis. *Contrib. Mineral. Petrol.*, 1987, **95**, 407–419.
27. Eby, G. N., The A-type granitoids: a review of their occurrence and chemical characteristics and speculations on their petrogenesis. *Lithos*, 1990, **26**, 115–134.
28. Frost, B. R., Barnes, C. G., Collins, W. J., Arculus, R. J., Ellis, D. J. and Frost, C. D., A geochemical classification for granitic rocks. *J. Petrol.*, 2001, **42**, 2033–2048.
29. Pearce, J. A., Harris, N. B. W. and Tindle, A. G., Trace element discrimination diagrams for the tectonic interpretation of granitic rocks. *J. Petrol.*, 1984, **25**, 956–983.
30. Suzuki, K., Adachi, M. and Tanaka, T., Precambrian provenance of Jurassic sandstone in the Mino terrane, central Japan: Th–U–total Pb evidence from an electron microprobe monazite study. *Sediment. Geol.*, 1991, **75**, 141–147.
31. Suzuki, K. and Adachi, M., Precambrian provenance and Silurian metamorphism of the Tsubonosawa paragenesis in the south Kitakami terrane, northeast Japan; revealed by the Th–U–total Pb chemical isochron ages of monazite, zircon and xenotimes. *Geochem. J.*, 1991, **25**, 357–376.
32. Suzuki, K. and Adachi, M., Middle Precambrian detrital monazite and zircon from the Hida gneiss on Oki–Dogo Island, Japan: their origin and implications for the correlation of basement gneiss of southwest Japan and Korea. *Tectonophysics*, 1994, **235**, 277–292.
33. Montel, J. M., Foret, S., Veschambre, M., Nicollet, C. and Provost, A., Electron microprobe dating of monazite. *Chem. Geol.*, 1996, **131**, 37–53.
34. Braun, I., Montel, J. and Nicollet, C., Electron microprobe dating of monazites from high-grade gneisses and pegmatites of the Kerala khondalite belt, southern India. *Chem. Geol.*, 1998, **146**, 65–85.
35. Santosh, M., Yokoyama, K., Biju-Sekhar, S. and Rogers, J. J. W., Multiple tectonothermal events in the granulite blocks of southern India revealed from EPMA dating: implications on the history of supercontinents. *Gondwana Res.*, 2003, **6**, 29–63.
36. Cocherie, A., Legendre, O., Peucat, J. J. and Kouamelan, A., *In situ* Th–U–Pb dating using an electron microprobe; a powerful tool for complex monazites. *Terr. Abstr.*, 1997, **9**, 441.
37. Steiger, K. and Jäger, E., Subcommission on geochronology: convention on the use of decay constants in geo-and cosmochronology. *Earth Planet. Sci. Lett.*, 1977, **36**, 359–363.
38. York, D., Least-squares fitting of a straight line. *Can. J. Phys.*, 1966, **44**, 1079–1088.
39. Bowles, J. F. W., Age dating of individual grains of uraninite in rocks from electron microprobe analyses. *Chem. Geol.*, 1990, **83**, 47–53.
40. Holmes, A., Radioactivity and geological time. *Natl. Res. Council Bull.*, 1931, **80**, 24–459.
41. Krogh, T. E., Improved accuracy of U–Pb zircon dating by selection of more concordant fractions using an air abrasion technique. *Geochim. Cosmochim. Acta*, 1982, **46**, 637–649.
42. Cherniak, D. J. and Watson, E. B., Pb diffusion in zircon. *Chem. Geol.*, 2000, **172**, 5–24.
43. Pandit, M. K. and Khatatneh, M. K., Geochemical constraints on anorogenic felsic plutonism in North Delhi Fold Belt, western India. *Gondwana Res.*, 1998, **2**, 247–255.
44. Pandit, M. K., Carter, L. M., Ashwal, L. D., Tucker, R. D., Torsvik, T. H., Jamtveit, V. and Bhushan, S. K., Age, petrogenesis and significance of 1 Ga granitoids and related rocks from the Sendra area, Aravalli craton, NW India. *J. Asian Earth Sci.*, 2003, **22**, 363–381.

ACKNOWLEDGEMENTS. We thank Ms Shigeoka for her help and guidance in sample preparation and microprobe analyses. P.K. acknowledges CSIR, New Delhi for Senior Research Fellowship and S.B.S acknowledges the Inoue Science Foundation, Japan for post-doctoral fellowship.

Received 8 April 2005; revised accepted 8 September 2005